Vibration Analysis of Heated Plates

B. O. Almroth,* J. A. Bailie,† and G. M. Stanley‡
Lockheed Missiles and Space Company, Inc., Sunnyvale, Calif.

A study has been carried out of the free vibrations of a solid-wing structure with a diamond-shaped profile. Vibration frequencies and modes are obtained at different levels of the temperature, which is distributed in a way that is typical for such wings at high speed. It is found that the lowest vibration modes are of local character for wings with elevated temperature. Large displacements in the local modes include membrane stresses, so flutter in such modes must be of limited amplitude. In addition, a very small imperfection in the midplane of the plate is sufficient to make the lowest frequencies relatively insensitive to thermal buckling. Thermal buckling of the leading edge, then, is not likely to change the aeroelastic properties of the wing severely.

Nomenclature

c = chord length, mm
P = force couple (Fig. 3)
T = temperature, °C
$\bar{T}$ = leading edge temperature, °C
$\bar{T}_{crit}$ = critical value of $\bar{T}$, °C
t = plate thickness, mm
x = chordwise distance from leading edge, mm
w = lateral displacement, mm
α = coefficient of thermal expansion
ω = vibration frequency, Hz
ω_0 = vibration frequency at zero temperature, Hz

Introduction

FOR reduction of drag, many platelike wing structures are designed with very thin edges (wedge- and diamond-shaped profiles). At high velocity, then, aerodynamic heating results in considerable temperature gradients. For the diamond-shaped profile, the temperature is high at the leading and trailing edges and has a minimum around midchord. The corresponding thermal stress field exhibits spanwise compression at the thin edges which must have a substantial effect on the stiffness of the wing and consequently on its aeroelastic behavior. Studies of this problem include the results of Refs. 1-5. These papers were published before the high-speed computer made detailed analysis of anything but very simple configurations possible.

The analytical solution presented in Ref. 2, for example, is based on a temperature distribution typical for the diamond-shaped profile but applied to a constant-thickness plate. It was assumed that the chord of the wing remains straight in buckling and vibration modes. Therefore, the results are somewhat approximate, even for the plate with constant thickness.

In Ref. 2, a temperature distribution is applied which varies parabolically in the chordwise direction, with a minimum at midchord. Degradation of the material properties is not accounted for. Hence it is sufficient to consider relative temperatures and to assign the temperature at midchord the value zero. The temperature at the leading edge measured in degrees Celsius will be denoted $\bar{T}$. In that case, thermal buckling for the constant-thickness plate occurs when

$$\bar{T} = \bar{T}_{crit} = 11.55 \quad t^2/(\alpha c^2)$$

Received May 23, 1977; revision received Aug. 18, 1977.
Index categories: Structural Dynamics, Aeroelasticity and Hydroelasticity.

*Senior Staff Scientist. Member AIAA.
†Staff Engineer. Member AIAA.
‡Scientist.

The buckling mode consists of a pure twisting of the plate. It coincides with the first torsional mode of vibration. As the temperature is increased, the frequency corresponding to this vibration mode decreases so that it vanishes at $\bar{T} = \bar{T}_{crit}$.

If the temperature is raised above its critical value, the plate begins to deform in the twisting mode. Corresponding postbuckling states are in stable equilibrium. The analysis of Ref. 2 indicates that the square of the vibration frequency corresponding to the first torsional mode decreases linearly (Fig. 1) until it becomes zero at the critical temperature. In the postbuckling range, the torsional stiffness increases with the temperature. If there is some initial distortion of the plate, the vibration frequency never will vanish completely, but it will pass through a minimum in the neighborhood of the cirtical temperature.

Thermal Buckling of Plate with Diamond-Shaped Profile

Attempts have been made also to analyze the more realistic case of wings with a variable plate thickness. Analyses predating the high-speed computer treated the wing as a simple beam clamped at the root chord generally assumed to have an infinite aspect ratio. In Ref. 6, Singer introduces an approximate correction for a finite aspect ratio. Computer solutions are presented in Ref. 7.

Here the results from a vibration analysis based on the STAGS computer program[8] are presented. (A brief description of STAGS is given in the Appendix.) A diamond-shaped wing as shown in Fig. 2 is considered. The wing is not clamped along the entire root chord, but (for relief of thermal stresses) sections at the forward and aft ends are free, as indicated in the figure. Similar results, presented in Ref. 7, are less accurate, as they are based on a rather coarse grid, and the number of points obtained for each curve is not quite sufficient to give a good picture of the trend of the frequencies in the immediate neighborhood of the critical temperature.

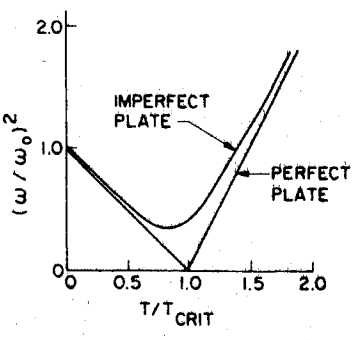

Fig. 1 Torsional mode frequency for plate with constant thickness.

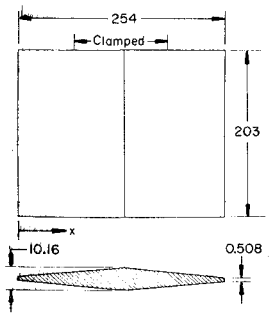

Fig. 2 Wing with diamond-shaped profile (dimensions in millimeters).

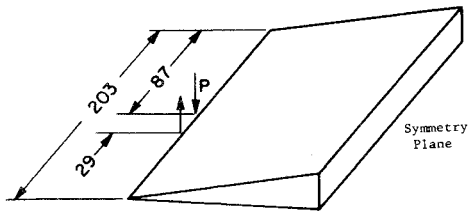

Fig. 3 Couple of lateral loads on half-wing (dimensions in millimeters).

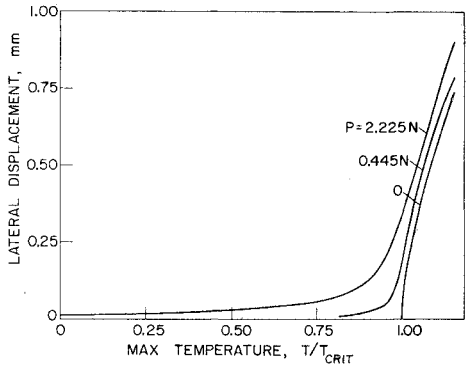

Fig. 4 Lateral displacement vs temperature.

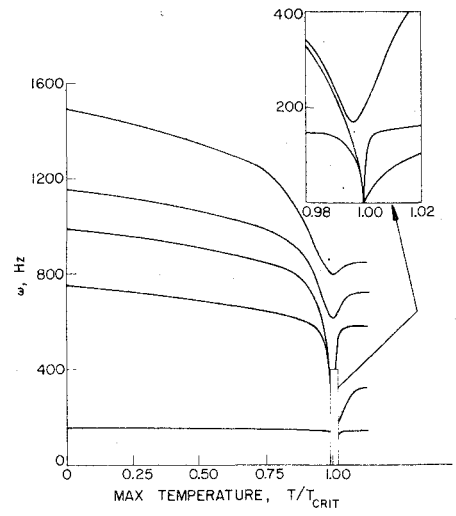

Fig. 5 Vibration frequencies for perfect wing: symmetric modes.

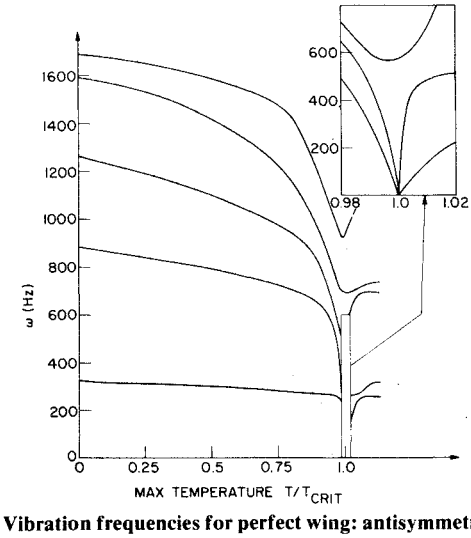

Fig. 6 Vibration frequencies for perfect wing: antisymmetric modes.

The results presented here are based on the temperature distribution

$$T = \bar{T}(2x/c - 1)^4$$

In the analysis of the basic stress state, advantage is taken of symmetry about a normal plane through the midchord. In the thermal buckling and in the vibration analyses, the modes are either symmetric or antisymmetric with respect to that plane.

For symmetric buckling, the lowest two eigenvalues are almost identical. The following critical values of the load factor were obtained: $\bar{T}_{crit} = 693.60$ °C and 693.68 °C. Use of antisymmetric boundary conditions in the buckling analysis gives eigenvalues of approximately the same size: $\bar{T}_{crit} = 693.55$ °C and 693.63 °C.

A nonlinear analysis was performed for wings with differing "degrees of imperfection." The imperfections were obtained through the application of lateral load couples at the leading and trailing edges, as shown in Fig. 3. This arrangement is the most convenient way to introduce imperfections in STAGS because definition of "stress-free imperfections" in the geometry requires that the program be recompiled for each configuration. The maximum lateral displacements as functions of the temperature factor are shown in Fig. 4 for $P = 0.0$, 0.445, and 2.225 N. At zero temperature, these forces correspond to very small lateral displacements. With $P = 2.225$ N, the maximum lateral displacement is only 0.036 mm. The postbuckling curve for the perfect plate ($P = 0$) is obtained by use of some point on a curve for an imperfect wing as a starting point. The lateral load P first is decreased to zero, and then the temperature is decreased gradually. Below the critical temperature, the equilibrium equations have unique solutions, and a configuration without lateral displacements is obtained.

The solutions of the nonlinear equations were utilized as a basic stress state in an analysis of small vibrations. The five lowest frequencies corresponding to symmetric modes are shown in Fig. 5 for the case of perfect plates ($P = 0$). We notice that two of the frequencies vanish at the critical temperature. This is expected, since at this point we have two almost identical roots to the bifurcation buckling problem. There is a very slight discrepancy between the critical temperature which is indicated by zero frequencies and by the bifurcation buckling analysis. This is because the effects of in-plane prebuckling rotations are omitted in the buckling analysis. The five lowest vibration frequencies for antisymmetric modes are shown in Fig. 6. As in the case with symmetric modes, two frequencies vanish at the critical temperature. At lower values of $\bar{T}$, the antisymmetric modes correspond to frequencies that are higher than those for symmetric modes.

The computer-generated plots in Figs. 7 and 8 show symmetric and antisymmetric modes for a few selected values of the temperature. Lines corresponding to zero displacement have been emphasized by hand, as otherwise the heavily reduced pictures would not give a clear indication of the deformation pattern. All of the modes shown become more

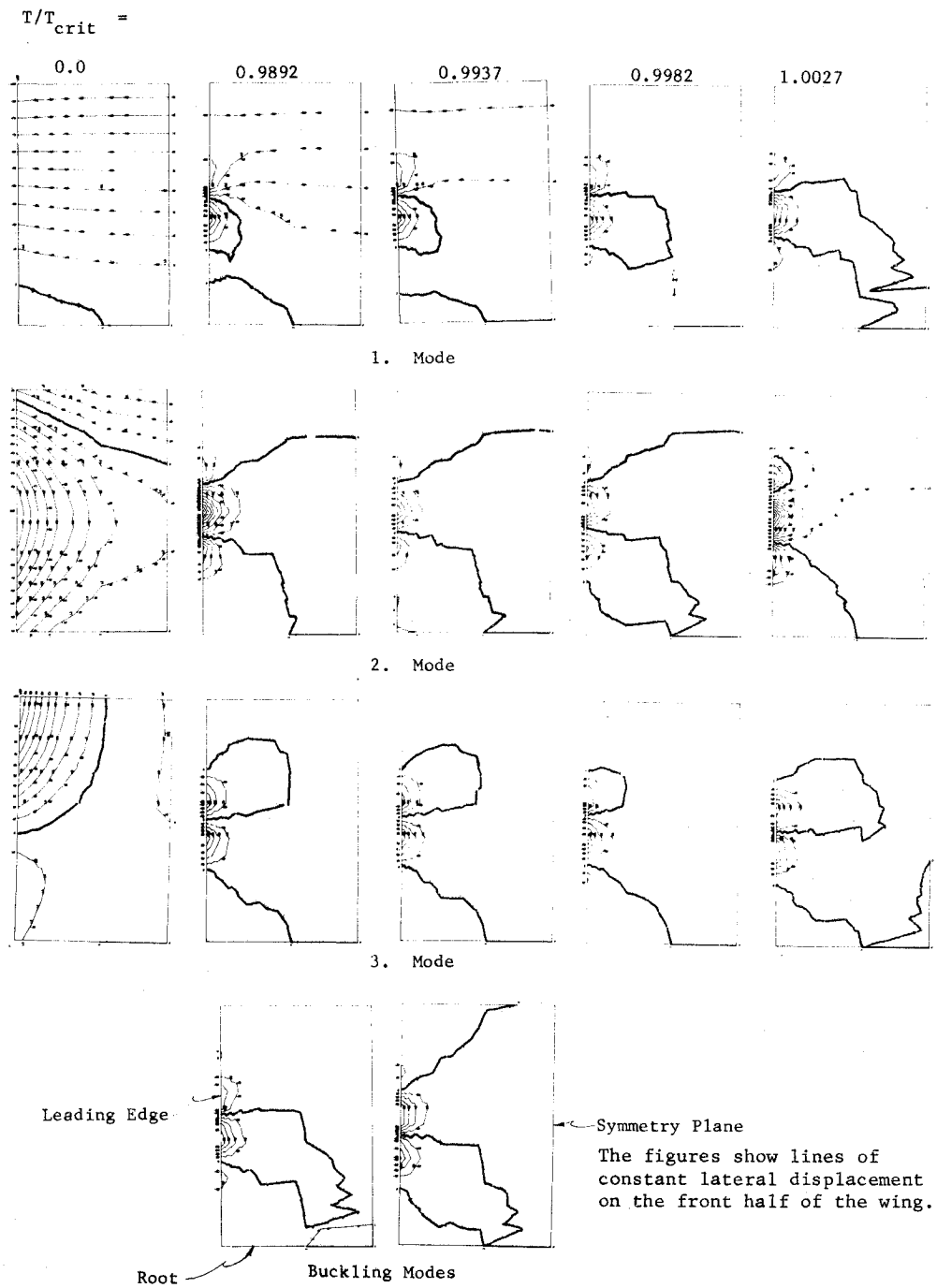

Fig. 7 Symmetric vibration modes.

localized when the temperature approaches its critical value. The two critical symmetric and antisymmetric buckling modes also are shown in the figures. The modes corresponding to the two lowest frequencies gradually are distorted with increasing temperature so that they coincide with the buckling modes at the critical temperature. That is, the frequency curves (Figs. 5 and 6) do not intersect one another for values of $\bar{T}$ less than $\bar{T}_{crit}$. However, the modes in Fig. 8 indicate that there is an exchange between the two lowest antisymmetric modes at $\bar{T}=\bar{T}_{crit}$.

If a small geometric imperfection is present or if small lateral loads are applied, there will not be a bifurcation in the load displacement curve or a temperature value at which the vibration frequencies will vanish. Figure 9 shows the symmetric frequencies for the two lowest symmetric modes in the presence of small imperfections. An imperfection so small that it hardly can be avoided in manufacturing (corresponding to $P=2.225$ N) is sufficient to erase completely the precipitous drop in frequency in the neighborhood of the critical temperature.

Conclusions

The typical temperature distribution for a diamond-shaped wing causes spanwise compressive stresses in the thin leading and trailing edges. Thermal buckling induced by these stresses make the edges very soft, and some vibration frequencies are very low in a small range around the critical temperature. However, these modes are local, and finite deformation will lead to stiffening membrane effects in contrast to the modes for the plate with constant thickness. Because of the stiffening effect of membrane forces, flutter in a local mode would have a low amplitude in the limit cycle.

The localized nature of the buckling mode and the presence of stiffening membrane forces also mean that the amplitude of the lateral displacement grows only slowly in the post-buckling range. Actually, computations show that, if the

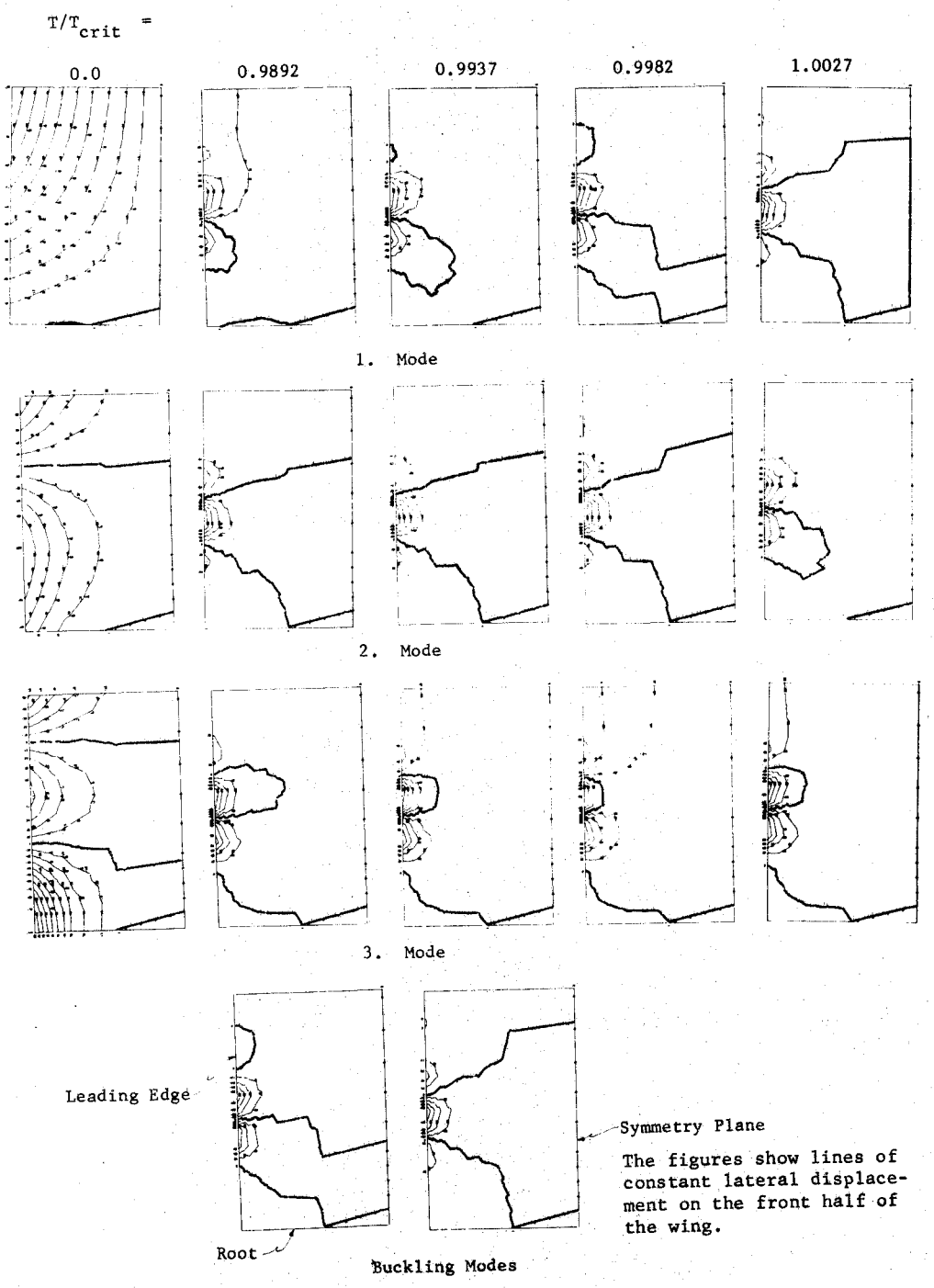

Fig. 8 Antisymmetric vibration modes.

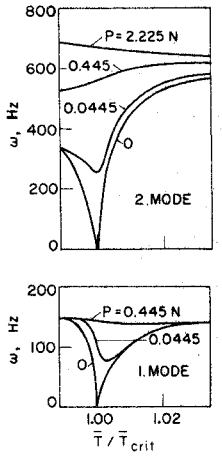

Fig. 9 Vibration frequencies for imperfect plates: symmetric.

degradation of elastic properties is taken into account, the amplitude of the buckling will grow to a maximum and then decrease. Since the buckle pattern covers a small part of the wing and the amplitude of the buckle remains relatively small, the occurrence of thermal buckling will be of little consequence on the deformation of the wing under steady aerodynamic effects.

The effect of small imperfections appears to be most important. Figure 9 shows that a very small imperfection still is sufficient to eliminate almost completely the drop in the lowest frequencies in the range around the critical temperature. Consequently, generalized forces and generalized masses will vary smoothly and relatively unperturbed through the range. Thermal buckling will, therefore, have a minor effect on the flutter velocity for a wing with some degree of imperfection. This is in sharp contrast to the behavior of the constant-thickness plate for which the frequency of the first

torsional mode becomes small in a range around the critical temperature.

Of course, the critical temperature for the diamond-shaped wing is much lower than it is for the wing with constant thickness. The present paper does not compare the aeroelastic behavior of the two types of plates. It only states that aeroelastic problems preclude flight patterns that would cause thermal buckling in one case but not in the other.

Appendix

STAGS is a computer code primarily intended for analysis of shell structures. The major interest has been in the nonlinear aspects of shell behavior. Therefore, much emphasis has been placed on computational efficiency. Under contract with NASA Langley, the computer code has been converted from being more or less a pure research tool into a code that is suitable for use in practical engineering analysis.

The capability of STAGS includes the following procedures: 1) linear stress analysis; 2) geometrically nonlinear elastic stress analysis; 3) inelastic stress analysis, geometrically linear or nonlinear; 4) bifurcation buckling analysis with linear or geometrically nonlinear prestress (elastic); 5) small vibration analysis with prestress based on linear or geometrically nonlinear analysis (elastic); and 6) transient response analysis, linear or geometrically nonlinear, elastic or inelastic. In a STAGS analysis, the structure can be defined as composed of a number of shell branches. Linear springs (axial or torsional) and nonlinear general beam elements also can be included. If the beams are defined as stiffeners attached to the shell along a line on its surface, appropriate displacement constraints will be enforced automatically. Loading is either mechanical (forces or forced displacements) or thermal. Only conservative force systems can be included. Any boundary conditions or other displacement constraints are permitted as long as they are linear.

Different finite-difference (energy method) or finite-element procedures are available as options for discretization of the shell branches. The finite-difference solution is based on the shell equations presented in Ref. 9. However, the analysis of flat plates presented here was based on a discretization with flat elements in which lateral displacements are bicubic and in-plane displacements at least quadratic. At each corner node, there are seven degrees of freedom: three displacement components, three rotation components, and the shear strain. In addition, displacements along the element boundaries are included as degrees of freedom at midpoint nodes, thus the total number of degrees of freedom per element is 32.

Bifurcation buckling and small vibration analyses lead to linear eigenvalue problems. In STAGS, these are solved through the generation of invariant subspaces by simultaneous power iteration.[10] Nonlinear static analysis results in nonlinear algebraic equations. For solution of such equations, the STAGS user has the options of using either the modified or the regular Newton method (cf. Ref. 11). For numerical integration, in transient analysis the following options are available: 1) the central difference scheme; 2) trapezoidal rule; 3) Gear's two- and three-order methods; or 4) Park's method. A discussion of these methods is available in Ref. 12.

Acknowledgment

The work reported here was funded by the Lockheed Missiles and Space Company, Inc., Independent Research Program. It is a direct extension of the work performed under contract with the Naval Air Development Center (N62269-73C-0713).

References

[1] Budiansky, B. and Mayers, J., "Influence of Aerodynamic Heating on the Effective Torsional Stiffness of Thin Wings," *Journal of the Aeronautical Sciences,* Vol. 23, Dec. 1956, p. 1081.

[2] Heldenfels, R.R. and Vosteen, L.F., "Approximate Analysis of Effects of Large Deflections and Initial Twist on Torsional Stiffness of a Cantilever Plate Subjected to Thermal Stress," NACA TR 1361, 1958.

[3] Biot, M.A., "Influence of Thermal Stress on the Aeroelastic Stability of Supersonic Wings," *Journal of the Aeronautical Sciences,* Vol. 24, June 1957, pp. 418-421.

[4] Kochanski, S.L. and Argyris, J.H., "Some Effects of Kinetic Heating on the Stiffness of Thin Wings," *Aircraft Engineering,* Oct. 1957, Feb. 1958, March 1958, and April 1958.

[5] Mansfield, E.H., "Combined Flexure and Torsion of a Class of Heated Thin Wings – A Large Deflection Analysis," R&M 3195, Aeronautical Research Council, London, March 1958.

[6] Singer, J., "Thermal Buckling of Solid Wings of Arbitrary Aspect Ratio," *Journal of the Aeronautical Sciences,* Vol. 25, Sept. 1958, pp. 573-580.

[7] Ericsson, L.E., Almroth, B.O., Bailie, J.A., Brogan, F.A., and Stanley, G.M., "Hypersonic Aeroelastic Analysis," Lockheed Missiles and Space Co., Rept. LMSC-D056746, 1975.

[8] Almroth, B.O. and Brogan, F.A., "The STAGS Computer Code," Lockheed Missiles and Space Co., Rept. LMSC-D558853, 1977.

[9] Almroth, B.O., Brogan, F.A., and Marlowe, M.B., "Collapse Analysis for Elliptic Cones," *AIAA Journal,* Vol. 9, Jan. 1971, pp. 32-37.

[10] Rutishauer, H., "Computational Aspects of F.I. Bauer's Simultaneous Iteration Method," *Numerische Mathematik,* Vol. 13, Jan. 1969, pp. 4-13.

[11] Almroth, B.O. and Felippa, C.A., "Structural Stability," *Proceedings of the International Symposium on Structural Mechanics Software,* Univ. of Maryland, College Park, Md., 1974, pp. 499-540.

[12] Park, K.C., "Practical Aspects of Numerical Time Integration," *Computers and Structures,* Vol. 7, June 1977, pp. 343-353.